Low power ovonic threshold switching characteristics of thin GeTe6 films using conductive atomic force microscopy

Anbarasu Manivannan, Santosh Kumar Myana, Kumaraswamy Miriyala, Smriti Sahu, and Ranjith Ramadurai

Citation: Applied Physics Letters **105**, 243501 (2014); doi: 10.1063/1.4904412
View online: http://dx.doi.org/10.1063/1.4904412
View Table of Contents: http://scitation.aip.org/content/aip/journal/apl/105/24?ver=pdfcov
Published by the AIP Publishing

Articles you may be interested in

Nanosecond switching in GeSe phase change memory films by atomic force microscopy
Appl. Phys. Lett. **104**, 053109 (2014); 10.1063/1.4863495

Phase change behaviors of Zn-doped Ge2Sb2Te5 films
Appl. Phys. Lett. **101**, 051906 (2012); 10.1063/1.4742144

A comparative study on electrical transport properties of thin films of Ge1Sb2Te4 and Ge2Sb2Te5 phase-change materials
J. Appl. Phys. **110**, 013703 (2011); 10.1063/1.3603016

Amorphous-to-crystalline phase transition of (InTe) x (GeTe) thin films
J. Appl. Phys. **108**, 024506 (2010); 10.1063/1.3457868

Phase-change characteristics of chalcogenide Ge 1 Se 1 Te 2 thin films for use in nonvolatile memories
J. Vac. Sci. Technol. A **25**, 48 (2007); 10.1116/1.2388956

Confidently measure down to 0.01 fA and up to 10 PΩ
Keysight B2980A Series Picoammeters/Electrometers
View video demo>
KEYSIGHT TECHNOLOGIES

This article is copyrighted as indicated in the article. Reuse of AIP content is subject to the terms at: http://scitation.aip.org/termsconditions. Downloaded to IP: 130.113.86.233 On: Tue, 10 Feb 2015 16:32:52

APPLIED PHYSICS LETTERS **105**, 243501 (2014)

Low power ovonic threshold switching characteristics of thin $GeTe_6$ films using conductive atomic force microscopy

Anbarasu Manivannan,[1,a)] Santosh Kumar Myana,[2] Kumaraswamy Miriyala,[2] Smriti Sahu,[1] and Ranjith Ramadurai[2,a)]
[1]*Discipline of Electrical Engineering, Indian Institute of Technology Indore, Madhya Pradesh, India*
[2]*Department of Material Science and Metallurgical Engineering, Indian Institute of Technology Hyderabad, Andhra Pradesh, India*

(Received 30 August 2014; accepted 5 December 2014; published online 15 December 2014)

Minimizing the dimensions of the electrode could directly impact the energy-efficient threshold switching and programming characteristics of phase change memory devices. A ∼12–15 nm AFM probe-tip was employed as one of the electrodes for a systematic study of threshold switching of as-deposited amorphous $GeTe_6$ thin films. This configuration enables low power threshold switching with an extremely low steady state current in the *on* state of 6–8 nA. Analysis of over 48 different probe locations on the sample reveals a stable Ovonic threshold switching behavior at threshold voltage, V_{TH} of 2.4 ± 0.5 V and the *off* state was retained below a holding voltage, V_H of 0.6 ± 0.1 V. All these probe locations exhibit repeatable *on-off* transitions for more than 175 pulses at each location. Furthermore, by utilizing longer biasing voltages while scanning, a plausible nano-scale control over the phase change behavior from as-deposited amorphous to crystalline phase was studied. © *2014 AIP Publishing LLC*. [http://dx.doi.org/10.1063/1.4904412]

Since the demonstration of reversible threshold switching properties of chalcogenide amorphous semiconductors,[1] a wide range of materials have fascinated experimentalists and theorists for decades to exploit them into numerous applications including information storage,[2] reconfigurable electronics[3] and solid state displays.[4] Notably, Phase change materials (PCM) have successfully facilitated commercially available optical storage products of various storage densities ranging from 650 MB (CD-R/W) to 50 GB (Blu-ray Disc). At the heart of this storage concept lies the fascinating property of reversible, quick transformation between amorphous and crystalline states on a nanosecond timescale triggered by an optical or electrical stimulus. This leads to a pronounced change of optical or electronic properties, which allow the storage of information.[2,5] This property together with relatively higher read/write speeds, low power consumption, high endurance and data retention makes them contenders for a high speed, non-volatile electronic memory, a plausible replacement to conventional flash memories.[6,7]

Consequently, there has been significant effort in recent years towards the improvement of programming characteristics: reliability, structural stability, and integration issues of PCM devices.[6,8] Also, novel PCM architectures have been developed to realize a cost-effective high-density memory.[9] Among the various criteria that make a memory technology promising, a key requirement is scalability. There are primarily two factors that are discerned when scalability is addressed: At first, the phase change material must retain its properties despite a reduction in its volume. Second, the space taken up by dielectrics and the electronics necessary to address and control the state of memory cell must be taken into account. In addition, the selector/access device essentially determines improvement on storage density of the conventional memory array. Recently, a novel architecture of vertically stackable cross-point PCM devices was demonstrated by employing a thin chalcogenide film as Ovonic Threshold Switch (OTS) selector device[1] for accessing programming of a storage element.[10] The OTS selector acts as an electronic switch to access the adjacent memory bit. The OTS selector device is expected to perform a stable threshold switching and *on-off* transitions at powers much lower than that required for phase change in the underlying storage element. This envisions a high-density three-dimensional memory via stacking of multiple layers of memory arrays capable of better scalability and compatible with even complementary metal-oxide semiconductor (CMOS) circuits.[10]

Therefore, significant effort has been made recently, to improve programming characteristics at extremely low powers using carbon nanotube (CNTs) as electrodes.[11] This reduction in dimension of the electrode could have the effect of power reduction as the contacts create a sizable electric field. Nevertheless, there is little information available regarding the electrode size dependency of threshold switching characteristics for low power operation, which is a major deficiency if one is interested in energy-efficient, scalable memories.

Hence, we have studied threshold switching properties of thin $GeTe_6$ films using a Conductive Atomic Force Microscope (C-AFM) having probe-tip diameter of ∼12–15 nm as one of the electrodes in contact mode of operation. We demonstrate the ability of as-deposited amorphous $GeTe_6$ thin films to manifest low power threshold switching at a critical voltage called threshold voltage, V_{TH} of 2.4 ± 0.5 V, with an extremely low *on* state current of 6–8 nA in the test cell structure. Further, we explored a nano-scale control over the phase change behavior from as-deposited amorphous to crystalline phase.

[a)]Authors to whom correspondence should be addressed. Electronic mail: anbarasu@iiti.ac.in and ranjith@iith.ac.in

 © 2014 AIP Publishing LLC

This article is copyrighted as indicated in the article. Reuse of AIP content is subject to the terms at: http://scitation.aip.org/termsconditions. Downloaded to IP: 130.113.86.233 On: Tue, 10 Feb 2015 16:32:52

Thin $GeTe_6$ films of 190 ± 1 nm thicknesses were deposited from a stoichiometric single target by dc magnetron sputtering (background pressure 2.5×10^{-6} millibar, 20 sccm Ar flow, deposition rate of 0.098 $nm.s^{-1}$, operating in constant power mode of 20 Watt) on 20×20 mm SiO_2 substrates. The amorphous nature of the as-deposited thin films was confirmed by x-ray diffraction. Compositional analysis of as-deposited $GeTe_6$ films performed by energy dispersive x-ray spectroscopic technique at over five locations reveals the ratio between Te to Ge as 5.5 ± 0.2.

The OTS characteristics of $GeTe_6$ thin films have been carried out using *Bruker multimode8* AFM operated in conductive mode. *Nanoscope V* controller and J scanner *AS-130VLR* were used for imaging. A ∼12–15 nm Probe-tip made of Sb doped Si with conductive coating of Pt/Ir was deployed in constant force mode with a force constant of 0.2 N/m for OTS experiments. The C-AFM module is capable of biasing voltage of up to 10 V and can measure currents ranging from a few pA up to 1 μA with the resolution of 3 pA. Prior to threshold switching measurements, the C-AFM module was calibrated with a standard specimen (highly oriented pyrolytic graphite, HOPG) supplied by *Bruker*, for the optimized scanning parameters.

The sample was then mounted on a metallic disc coupled with the sample holder. The schematic diagram of the experimental setup is shown in Figure 1(a). A conductive path was established using silver paste with the substrate. The surface morphology of $GeTe_6$ films was recorded with biasing voltages of 1–2 V, during which no significant current flow was observed above a few pA. This is indicative of the highly resistive amorphous nature of the films. The RMS roughness of the sample was found to be 1.25 nm. The voltages used to study the morphology of as-deposited amorphous phase were carefully chosen such that they are actually less than the threshold voltage of $GeTe_6$ films.

I-V characteristics and threshold switching experiments of $GeTe_6$ films were carried out using ramping voltage pulse of 0–3 V and the resultant current was measured, during which the probe-tip was kept stationary in C-AFM configuration. Figure 1(b) displays the I-V characteristics and the OTS behavior of thin $GeTe_6$ films. The applied ramping voltage of 0 to 3 V and measured currents (leading edge: black color, trailing edge: red color) possess a 2 ms delay time between each data points. As can be seen, the device remains in the highly resistive *off* state until a specific electrical voltage value, known as the threshold voltage, V_{TH} of 2.4 ± 0.5 V, beyond which the device switches to a conducting *on* state. The steady state current in the *on* state was found to be approximately 6–8 nA for the applied voltage of 3 V. Upon removal of the applied voltage, the device remains in the conducting *on* state, until a critical voltage, called holding voltage V_H, below which the device goes back to its initial high resistive amorphous state as evidenced by the device current reaching a value of zero at a holding current, I_H corresponding to V_H. Figure 1(c) depicts an enlarged view of the *on* to *off* transition via the holding voltage. The holding voltage, V_H was measured to be as 0.6 ± 0.1 V, which matches well with previous studies.[12] It is noteworthy that the device remains in the *on* state until the applied voltage is reduced to the holding voltage which confirms the OTS behavior and the *on-off* transitions. The OTS behavior and the *on-off* transitions were found to be reproducible for more than 175 pulses on the same location without retracting the probe-tip.

In order to further examine the stability and reproducibility of the OTS behavior, similar experiments of I-V characteristics and OTS behavior were systematically performed on 48 different probe points. The OTS behavior was testified on each probe point, which was selected by moving the probe-tip in an appropriate direction on a 500×500 nm region as depicted in Figure 2(a). The signatures of OTS and *on-off* transitions were confirmed in all the probe locations. Repeatable OTS behavior was observed at each probe location for more than 175 pulses without retracting the probe-tip. The spread in V_{TH} of 2.4 ± 0.5 V on these probe locations are shown in Figure 2(b). Subsequent scanning of the surface morphology after these experiments was observed to be the same as that prior to the OTS experiments. This confirms that there were no structural changes by means of applied voltage pulses on amorphous phase upon *on-off* transitions.

The OTS results of $GeTe_6$ films using C-AFM reported here is in accordance with experimental results on a time-resolved nanosecond threshold switching as described in the literature.[12] Also, these devices have shown a steady state

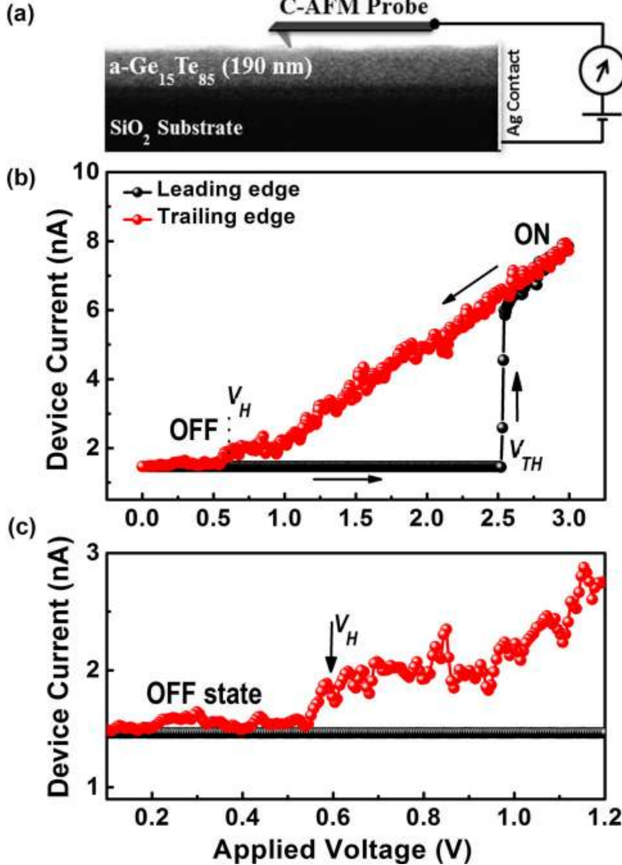

FIG. 1. (a) Schematic of C-AFM set-up used for performing the OTS behavior and *on-off* characteristics. (b) I–V characteristics and OTS behavior of $GeTe_6$ thin films for the applied electric voltage of 3 V. (c) Enlarged view of *on* to *off* transition via holding voltage $V_H \sim 0.6 \pm 0.1$ V at which device current goes to zero.

This article is copyrighted as indicated in the article. Reuse of AIP content is subject to the terms at: http://scitation.aip.org/termsconditions. Downloaded to IP: 130.113.86.233 On: Tue, 10 Feb 2015 16:32:52

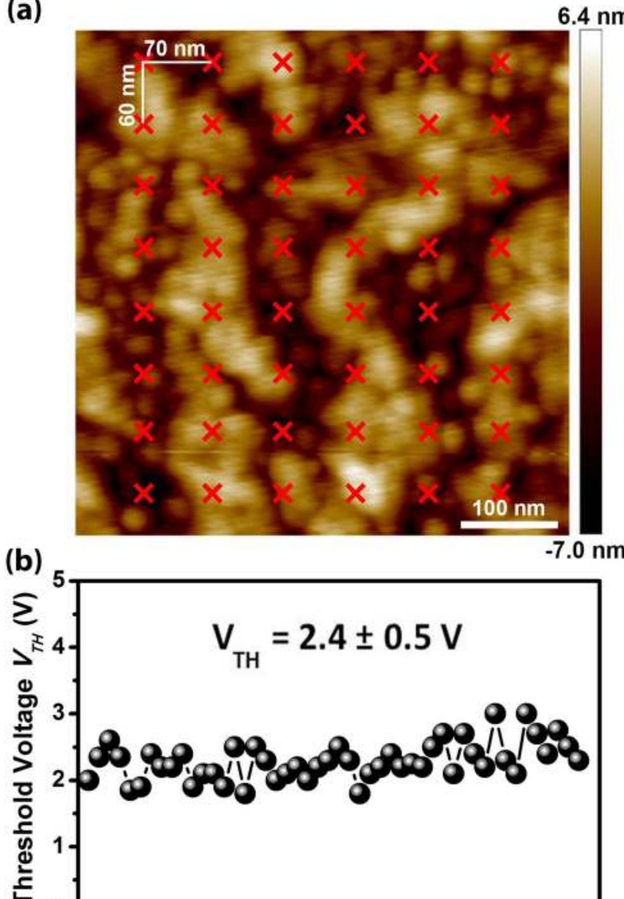

FIG. 2. (a) Surface morphology of a 500 nm region $GeTe_6$ thin films indicating 48 probe points at which threshold switching and *on-off* transitions were carried out by systematically varying 70 nm in X-direction and 60 nm in Y-direction. (b) Distribution of threshold voltage, V_{TH} of 2.4 ± 0.5 V on 48 various probe points.

current in the *on* state of ∼400 μA for the applied voltage of 1.9 V in a classical bottom heater geometry as reported elsewhere.[8]

The mechanism of threshold switching[13] has generated research interest for more than four decades, the intent mainly being to understand the various aspects of threshold switching phenomena including the primary reason for the initiation of the switching process,[14] such that whether it comprises purely electronic or thermal effects, transient *on* and *off* state characteristics, switching kinetics, the nature of the *on* state, and recovery properties.[15,16] Voltage pulse measurements on various device configurations revealed the aforementioned important aspects describing the switching mechanism. In particular, the nature of electronically sustained *on* state as a function of film thickness, pore size, and electrode material were studied using various measurement techniques including velocity-saturation effects, high frequency measurements, transient *on*-state characteristics (TONC), and pore-saturation effects.[15,17] These results have clearly revealed the dependence of filament radius as a function of steady state current. A theoretical framework of secondary phase conductive filaments has corroborated with the experimental data of the dependency of steady state current with filament radius and was found to be in good agreement with analytical results.[18] This information has recently regained interest in connection with the selection of OTS selector devices in a vertically stackable cross-point memory architecture[10] to realize a scalable, high-density PCM. Hence, information on OTS behavior with smaller electrode configurations is considerably important for better programming characteristics upon device scaling.

In-line with this, the present experimental results show the steady state current in the *on* state of approximately 6–8 nA, for the applied voltage pulse of 3 V, over the conducting area of the AFM probe-tip sized 12–15 nm. As it is encouraging to testify the scalability of the observed parameters, we made an attempt to evaluate their scaling with the dimensions of electrode by considering it as a conducting filament radius with steady state current in the *on* state of the OTS devices. Moreover, the filament radius was calculated analytically based on the theoretical calculations reported elsewhere.[18] The filament radius was analytically calculated as 17.46 nm for 6 nA and 20.17 nm for 8 nA of steady state current in the *on* state. Figure 3 displays a viewgraph drawn with respect to the filament radius versus the steady state current of several electrode sizes and configurations reported elsewhere[13,14,18] with the present experimental, analytical data. It is interesting to note here that the steady state current in the conducting *on* state of the threshold switching device is decreasing upon the size of the electrode dimensions. Also, it is noteworthy to mention here that the present data typically conform that the steady state current is proportional to the square of the filament radius as reported in the literature.[18] With this understanding, the results presented here demonstrate more than three orders of lower steady state current observed upon reducing the electrode size as compared to previous studies and also found to be in good agreement.

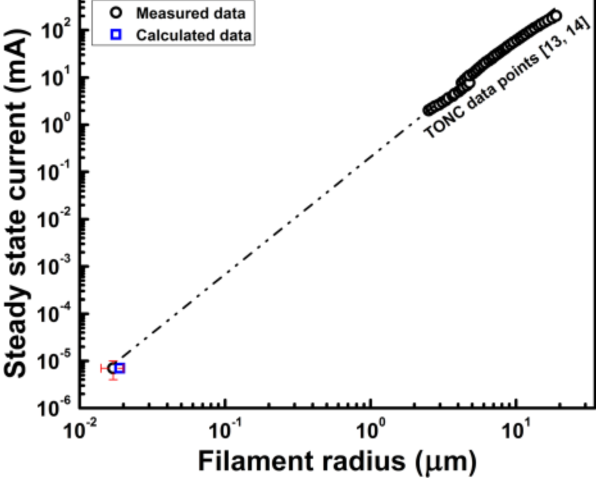

FIG. 3. Filament radius as a function of steady-state current in the *on* state, all the data points, except this work, were reproduced from the previous reports.[13,14] The filament radius (marked as square symbol) was calculated analytically based on the literature.[18] A very good agreement is obtained between the analytical value calculated with data and also consistent with the relationship of the steady state current is proportional to the square of filament radius.

This article is copyrighted as indicated in the article. Reuse of AIP content is subject to the terms at: http://scitation.aip.org/termsconditions. Downloaded to IP: 130.113.86.233 On: Tue, 10 Feb 2015 16:32:52

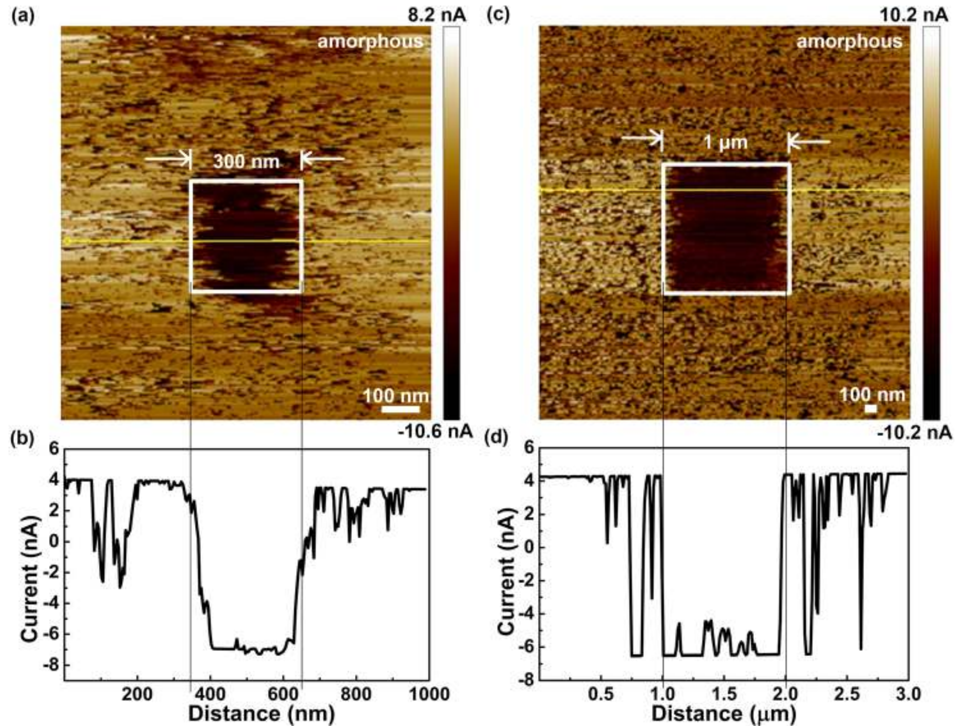

FIG. 4. (a) AFM topography image showing a crystallized region of 300 nm in a 1 μm as-deposited amorphous $GeTe_6$ film. (b) Current images recorded with a biasing voltage of 1 V showing a significant increase in the current due to reduction in the resistances on the size of crystalline marks. (c) AFM topography image showing crystallized region of 1 μm in a 3 μm as-deposited amorphous $GeTe_6$ film. (d) Current images recorded along the line profile with a biasing voltage of 1 V showing a significant increase in the current due to reduction in the resistances on the size of crystalline marks.

Increasing the *on* state current allows the crystallization of the conducting channel accomplishing a memory switching behavior known as *set* state in PCM devices.[19,20] This would be helpful in identifying the currents responsible for the onset of memory switching. Therefore, we examined a nanoscale control on memory switching behavior by electrically induced phase change from amorphous to crystalline state. A series of scanning with longer electrical pulses (more than 100 ms between each data points) were applied while maintaining a slow scanning speed as necessitated by the fact that $GeTe_6$ materials exhibit slow crystallization upon electrical/optical stimulus. Hence, a chosen value (based on the V_{TH}) of 3 V longer biasing is used for inducing the phase change from amorphous to crystalline state, whereas a chosen value of 1 V was used to read the information by scanning a slightly larger area of the morphology of the sample, so as to identify the crystalline mark on the amorphous background.

Figure 4(a) displays a nanoscale control of the crystalline mark sized 300×300 nm made while scanning by means of applying longer voltage pulse of 3 V. The crystallized region was evidently seen in the amorphous background upon scanning of surface morphology of 1 × 1 μm area using read voltage pulses (1 V biasing). Figure 4(b) depicts the current profile on a row of the entire amorphous matrix inclusive of conductive crystalline marks that reveal an enhanced current of 11 nA on the crystallized region due to their low resistance compared to the amorphous matrix. This clearly indicates memory switching induced by electrical pulses as evidenced by nano-sized crystallized region in the amorphous matrix. Further, to support this, subsequently similar experiments were made on the entire area of 1 × 1 μm, which was scanned with a higher biasing voltage of 3 V in order to realize the phase transition. The crystallized region was then obtained by scanning a slightly larger area of 3 × 3 μm as shown in Figure 4(c). Furthermore, a corresponding current profile as displayed in Figure 4(d) evidently shows a crystallized region of 1 μm as revealed by the enhanced sample current of 11 nA due to low resistance when compared with the amorphous phase. The electrical energy supplied to the electrode was approximately 1.4 nJ for memory switching which was found to be more than two orders of magnitude higher as compared to the energy supplied for threshold switching (calculated as 12.6 pJ) on $GeTe_6$ thin films as per the above-mentioned device configuration. This higher energy for memory switching was achieved due to longer time delay of 100 ms between two data points. Hence, a clear nanoscale control on crystallization over amorphous matrix was obtained. It is noteworthy from Figure 4 that the bias voltage of 3 V induced the crystallized marks to whole region of 300 nm as well as 1 μm. It is unambiguously evident that the conductive crystalline region was observed in the current mapping image. Thus, the memory switching behavior indicating the structural change from amorphous to crystalline phase of $GeTe_6$ films by means of suitable longer, higher voltage pulses is evident. This signature of memory switching is in good agreement with previous C-AFM measurements on Sb rich amorphous $Ge_2Sb_{2+x}Te_5$ films.[17] Nevertheless, our study on nanoscale memory switching characteristics using C-AFM required longer voltage pulses as compared with previous studies.[17] This is necessitated owing to the fact that the eutectic composition $GeTe_6$ as a good glass former possesses better thermal stability, due to which, a slow crystallization process (crystallization time of more than 100 μs) was observed by means of laser-induced crystallization.[21,22] This is the clear evidence that the crystallization of $GeTe_6$ films is impossible by means of nanosecond pulses. Further improvements on the optimization of a stable glass composition with various material combinations might help to advance reliability and performance characteristics of the OTS device.[23] Therefore, it is noteworthy to mention here that the OTS

This article is copyrighted as indicated in the article. Reuse of AIP content is subject to the terms at: http://scitation.aip.org/termsconditions. Downloaded to IP: 130.113.86.233 On: Tue, 10 Feb 2015 16:32:52

devices could be envisioned for numerous applications including reconfigurable electronics and logic circuits.[24]

In summary, we have demonstrated low power threshold switching and *on-off* characteristics of as-deposited amorphous thin $GeTe_6$ films using a 12–15 nm C-AFM probe-tip as one of the electrodes. This demonstrates an extremely low steady state current in the *on* state of 6–8 nA upon the applied voltage V_{TH} of 2.4 ± 0.5 V. OTS experiments at various probe locations confirm a repeatable threshold switching and *on-off* transitions for more than 175 pulses at each location. In addition, scaling of electrode dimension reveals that the steady state current is proportional to the square of the filament radius. Furthermore, a nano-scale control over the phase change behavior of thin $GeTe_6$ films from as-deposited amorphous to crystalline phase was demonstrated.

M.A. thanks the Department of Science and Technology for financial support (Grant No. SERB/F/0894/2013-14). We acknowledge valuable discussions with S. Murugavel.

[1]S. R. Ovshinsky, Phys. Rev. Lett. **21**, 1450 (1968).
[2]M. Wuttig and N. Yamada, Nat. Mater. **6**, 824 (2007).
[3]M. H. R. Lankhorst, B. W. S. M. Ketelaars, and R. A. M. Wolters, Nat. Mater. **4**, 347 (2005).
[4]P. Hosseini, C. D. Wright, and H. Bhaskaran, Nature **511**, 206 (2014).
[5]D. Lencer, M. Salinga, and M. Wuttig, Adv. Mater. **23**, 2030 (2011).
[6]H. S. Philip Wong, S. Raoux, S. B. Kim, J. Liang, J. P. Reifenberg, B. Rajendran, M. Asheghi, and K. E. Goodson, Proc. IEEE **98**, 2201 (2010).
[7]D. Loke, T. H. Lee, W. J. Wang, L. P. Shi, R. Zhao, Y. C. Yeo, T. C. Chong, and S. R. Elliot, Science **336**, 1566 (2012).
[8]S. Lai and T. Lowrey, Tech. Dig. - Int. Electron Devices Meet. **2001**, 36.5.1.
[9]F. Pellizzer, A. Pirovano, F. Ottogalli, M. Magistretti, M. Scaravaggi, P. Zuliani, M. Tosi, A. Benvenuti, P. Besana, S. Cadeo, T. Marangon, R. Morandi, R. Piva, A. L. Spandre, R. Zonca, A. Modelli, E. Varesi, T. Lowrey, A. Lacaita, G. Casagrande, P. Cappelletti, and R. Bez, Tech. Dig. Symp. VLSI Technol. **2004**, 18.
[10]D. C. Kau, S. Tang, I. V. Karpov, R. Dodge, B. Klehn, J. A. Kalb, J. Strand, A. Diaz, N. Leung, J. Wu, S. Lee, T. Langtry, K. Chang, C. Papagianni, J. Lee, J. Hirst, S. Erra, E. Flores, N. Righos, H. Castro, and G. Spadini, Tech. Dig. - Int. Electron Devices Meet. **2009**, 617.
[11]F. Xiong, A. D. Liao, D. Estrada, and E. Pop, Science **332**, 568 (2011).
[12]M. Anbarasu, M. Wimmer, G. Bruns, M. Salinga, and M. Wuttig, Appl. Phys. Lett. **100**, 143505 (2012).
[13]D. Adler, M. S. Shur, M. Silver, and S. R. Ovshinsky, J. Appl. Phys. **51**, 3289 (1980).
[14]K. E. Petersen and D. Adler, Appl. Phys. Lett. **27**, 625 (1975).
[15]D. Adler, H. K. Henisch, and N. F. Mott, Rev. Mod. Phys. **50**, 209 (1978).
[16]D. Ielmini, Phys. Rev. B **78**, 035308 (2008).
[17]K. E. Petersen and D. Adler, J. Appl. Phys. **47**, 256 (1976).
[18]V. G. Karpov, M. Nardone, and M. Simon, J. Appl. Phys. **109**, 114507 (2011).
[19]R. Pandian, B. J. Kooi, G. Palasantzas, and J. T. M. De Hosson, Adv. Mater. **19**, 4431 (2007).
[20]J. L. Bosse, I. Grishin, Y. G. Choi, B.-k. Cheong, S. Lee, O. V. Kolosov, and B. D. Huey, Appl. Phys. Lett. **104**, 053109 (2014).
[21]M. Chen, K. A. Rubin, and R. W. Barton, Appl. Phys. Lett. **49**, 502 (1986).
[22]S. Raoux, H. Y. Cheng, M. A. Caldwell, and H. S. Philip Wong, Appl. Phys. Lett. **95**, 071910 (2009).
[23]H.-W. Ahn, D. S. Jeong, B.-k. Cheong, H. Lee, H. Lee, S.-d. Kim, S.-Y. Shin, D. Kim, and S. Lee, Appl. Phys. Lett. **103**, 042908 (2013).
[24]W. Czubatyj and S. J. Hudgens, Electron. Mater. Lett. **8**, 157 (2012).

This article is copyrighted as indicated in the article. Reuse of AIP content is subject to the terms at: http://scitation.aip.org/termsconditions. Downloaded to IP: 130.113.86.233 On: Tue, 10 Feb 2015 16:32:52